



# Diffraction Pattern Simulation of Crystal Structure towards the Ionic Radius Changes Via Vesta Program

*Ari Sulisty Rini<sup>1</sup> and Sundami Restiana<sup>2</sup>*

<sup>1,2</sup> Department of Physics, Faculty of Mathematics and Natural Sciences, Universitas Riau

**Abstract.** The Simulations of X-ray diffraction patterns of MgO, BaO and ZnS ceramics were successfully performed by VESTA program, based on the crystal structures visualization. The aim of this research was to obtain the relationship between ionic radius to the diffraction pattern. The X-ray diffraction pattern was generated from visualization of the crystal structure. The crystal structure information was obtained from JCPDS data which contained lattice parameter, atomic coordinate and the space group. The X-ray diffraction pattern parameters which are taken into account in this research are diffraction angle of 2 Theta and Intensity. The results indicated that the peak position and intensity of the diffraction pattern are influenced by ionic radius of the cations. Structural transformation was also detected from this simulation.

**Keyword:** Visualization, Simulation, X-ray diffraction, and VESTA

Received 16 April 2019 | Revised [17 July 2019] | Accepted [31 August 2019]

## 1 Introduction

The structure of a crystal plays an important role in material characterization. Knowledge of the crystal structure of a material can indirectly provide information about the properties of materials [1-3]. XRD is the most basic and most widely used material structure characterization method for analyzing the structure of solid crystals. This technique can identify the crystalline phase of the material, the crystal structure and the microstructure phase [4-7]. The information needed in determining the crystal structure is the lattice constant, and the space group adopted. Both of these information can be used to determine the position of an atom in a unit cell of a crystalline material.

Determining the structure using XRD applies the scattering principle that meets the Bragg Law which will give the position of the diffraction peak angle. According to Bragg, constructive interference occurs when the length of the path taken by scattering rays is parallel or the difference in the light trace must be an integer multiple of the wavelength ( $\lambda$ ) which can be written in the following equation [8-11].

---

\*Corresponding author at: Jl. Prof. Muchtar Luthfi Pekanbaru, 28293, Indonesia

E-mail address: ari.sulisty@lecturer.unri.ac.id

$$n\lambda = 2 d_{hkl} \sin \theta \quad (1)$$

In simple cube crystals with miller index (hkl) and lattice length, the distance between dhkl fields can be written as follows [12-13]:

$$d_{hkl} = \frac{a}{\sqrt{h^2 + k^2 + l^2}} \quad (2)$$

All atoms in the lattice contribute to scattering based on the position (x, y, z) of each constituent atom which is defined as a structural factor by the following formula:

$$F = \sum_n f_n e^{2\pi i(h\hat{x} + k\hat{y} + l\hat{z})} \quad (3)$$

Where the intensity is  $I \sim |F|^2$ . Diffraction beam intensity does not only depend on the structure factor  $|F|^2$ , but there are other factors, namely multiplicity (P), Lorentz polarization factor (L), and temperature factor ( $e^{-2M}$ ) [5].

$$I = F^2 \cdot P \left( \frac{1 + \cos^2 2\theta}{\sin^2 \theta \cos \theta} \right) e^{-2M} \quad (4)$$

The effect of ionic radius of cations has different responses to the intensity of each diffraction peak angle. This is due to several factors that influence the intensity of diffraction, namely multiplicity (multiplying factor), Lorentz polarization factors, temperature factors and absorbs. The multiplier comes from repeating the number of identical fields, the absorption factor depends on the geometry and diffraction method used, while the Lorentz polarization factor ( $L = \frac{1 + \cos^2 2\theta}{\sin^2 \theta \cos \theta}$ ) is a function of  $\theta$  whose value varies greatly with the angle Bragg. The value of the Lorentz polarization factor considers certain geometric factors related to the orientation of the reflecting plane in the crystal which also affects the diffraction intensity [14]

The diffraction peaks of a material often shift from standard data. In this study, VESTA software was used to determine the lattice parameters of a material through visualizing the structure of the material. VESTA uses the C++ programming language based on OpenGL technology with the ability to analyze the structure and electronic properties of a material [15-17].

Another factor that affects the intensity of a diffraction pattern is the difference in the number of lattices in one cluster which has implications for the difference in the size of the reference sample crystallite with simulation data, so that it can explain the difference in the intensity of each diffraction pattern of the same compound.

The VESTA software is commonly used to visualize crystal structures based on lattice parameter data and constituent atomic coordinates. Crystal structure visualization is increasingly

popularly to explain electrical phenomena from a material, and the description of structural transformation [18-19] and [20]. The zeolite mineral visualization has also been carried out using the VESTA program to increase the understanding of the composition of the mineral content. In this research, the VESTA program was used to simulate X-ray diffraction patterns of several ceramics such as MgO, BaO and ZnS through visualization of their structure by varying their ionic cation radius ( $M^{n+}$ ). The purpose of this research was to obtain a relationship between the displacement of the diffraction peak angle and its lattice parameters which had previously been validated.

## 2 Materials and Methods

The research was conducted by simulating the diffraction pattern of BaO, MgO and ZnS ceramics with ionic radius variations of cations. The ceramic data used was obtained from the JCPDS (Joint Committee on Powder Diffraction Standard) database of the MATCH!3 software which has been validated and can be traced to the origin of the data. The JCPDS data contains lattice parameter data, space groups, diffraction patterns and atomic coordinates in the grid. Crystal structure data used in this simulation are shown in Table 1.

**Table 1.** Ionic radius and lattice parameter of crystal structure

Ceramics	Cation radius ( $M^{n+}$ )	Anion radius ( $A^{n-}$ )	Lattice parameter, a (Å)	Space group	No. JCPDS
MgO	0.72	1.40	a= 4.144	Fm3m	96-901-3196
BaO	1.42	1.40	a = 4.397 c = 3.196	P4/nmm	96-152-7736
ZnS	0.74	1.84	a =5.345	Fm3m	96-500-0089

The research flowchart is displayed in the figure below

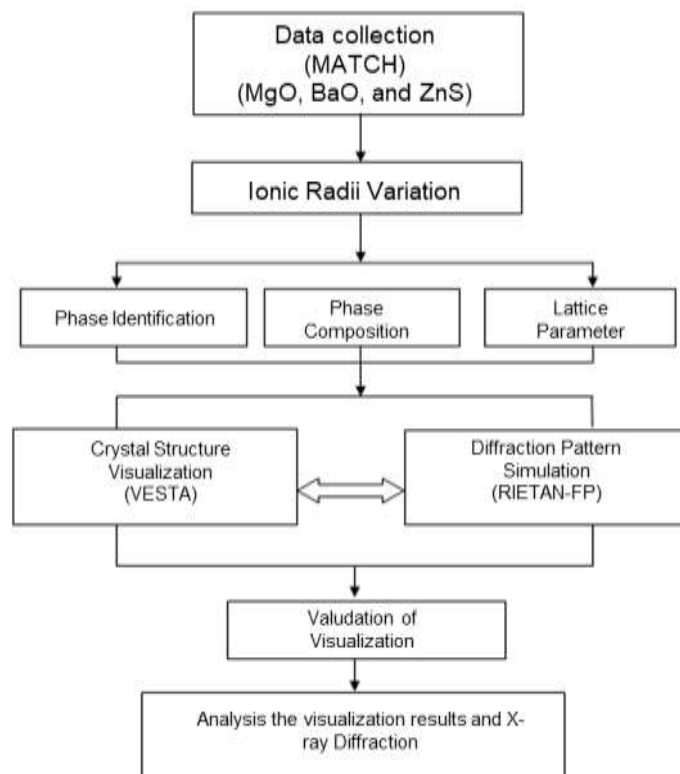


**Figure 1.** Research Flowchart

The X-ray diffraction patterns were obtained after visualization of the crystal structure was performed. Validation of crystal structure accuracy was conducted by comparing the diffraction patterns of the simulation results with the standard JCPDS data.

The simulation phase is as follows:

1. Composite atomic input, and lattice parameter
2. The constituent atomic coordinates in the grid input
3. Space group input
4. Visualization
5. “Powder Diffraction Pattern”

### 3 Result and Discussion

Visualization of the crystal structure was first validated by comparing the simulation results of X-ray diffraction patterns and reference patterns of ceramic materials. In this reserch, the validation data displayed is only MgO data. The results of visualization of crystal structures and ceramic diffraction patterns of MgO, BaO and ZnS are shown in Figure 2. The accuracy test of visualization was conducted by comparing the diffraction patterns of the simulation results with the JCPDS standard reference diffraction pattern. The simulation results of X-ray diffraction patterns of MgO, BaO and ZnS compounds that were made reveal the compatibility between the peaks of the simulation results with the tops of the JCPDS standard reference data, meaning that the visualization made is correct.

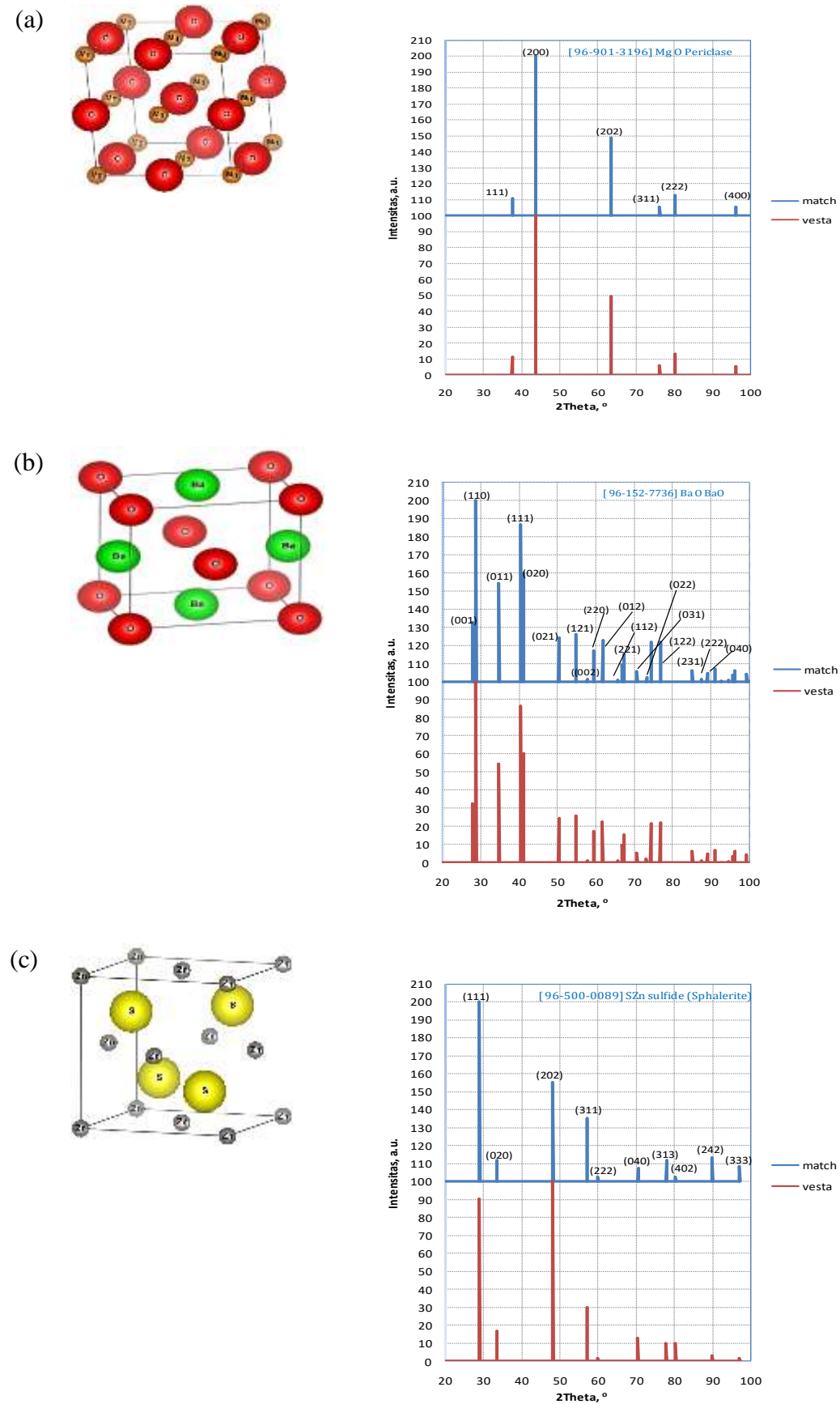


**Figure 2.** The crystal structure visualization and diffraction patterns of (a) MgO, (b) BaO, (c) ZnS

The data displayed for validation is from MgO with JCPDS number of 96-901-3196. The comparison of  $2\theta$  angle and the intensity of the diffraction pattern of the MgO compound from the simulation results with reference are described in Table 2.

**Table 2.** The comparison of  $2\theta$  value and simulation intensity to the references

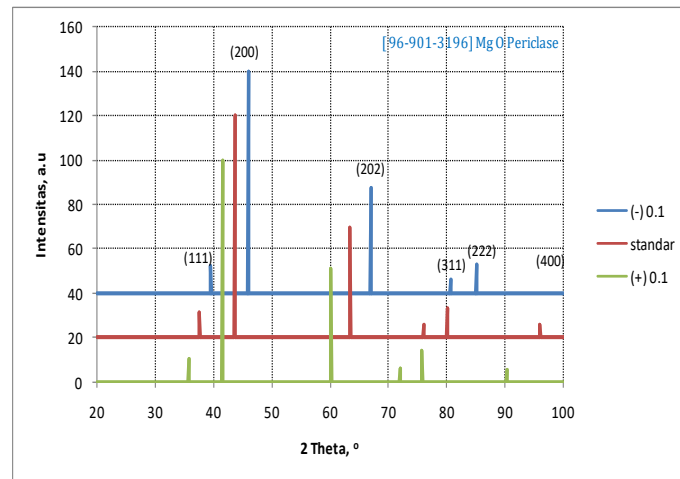
$2\theta$ (°)		% difference $2\theta$	I (a.u)		% difference I
Simulation	References		Simulation	Reference	
37.562	37.573	0.029	11.496	10.94	5.08
43.648	43.661	0.030	100	100	0.00
63.438	63.458	0.032	49.411	49.0	0.84
76.122	76.143	0.028	5.988	5.7	5.05
80.168	80.191	0.029	13.275	13.03	1.88
96.065	96.099	0.035	5.649	5.5	2.71
Mean		0.030	Mean		2.59

The scattering  $2\theta$  angle simulation results are found to coincide with references. The difference in the calculation of the simulation results with references in percentage is calculated using the following formula.

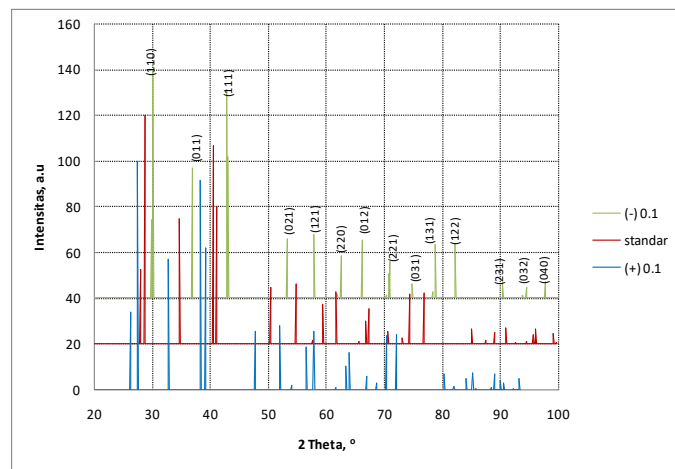
$$\% \text{ difference} = \left| \frac{\text{Value}_{\text{references}} - \text{Value}_{\text{simulation}}}{\text{Value}_{\text{reference}}} \right| \times 100 \% \quad (5)$$

The value of  $2\theta$  angle difference simulation results with reference is 0.030% while the difference in the intensity value of the simulation results with reference is 2.59%. The difference in the angle of  $2\theta$  the reference pattern and the pattern of the simulation results are relatively very small and it can be said that the visualization is very precise. The difference in the intensity value of diffraction peaks is due to the reference pattern derived from X-ray diffraction by crystals that are not ideal, while the diffraction pattern of the simulation results comes from the calculation of the ideal single crystal scattering pattern.

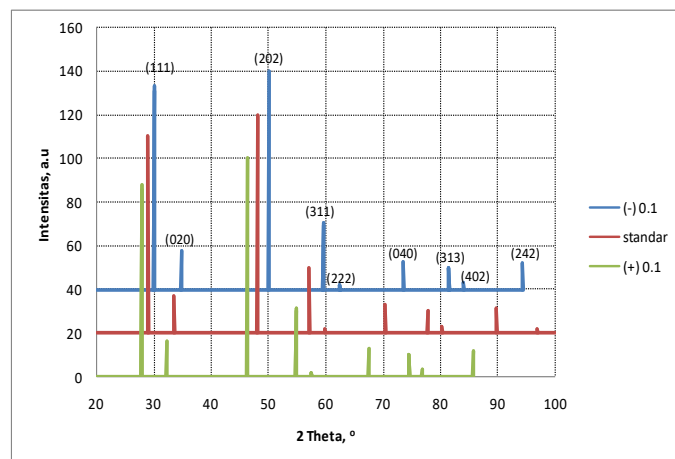
The standard diffraction pattern (without increase and decrease in cation radius) of MgO, BaO and ZnS compounds was then analyzed based on the ionic radius of cations and anions as shown in Figure 3. Based on the visualization of standard structures, it can be analyzed that the ionic radius of the atom affects the shape of the structure as well as the pattern of diffraction peaks.



(a)



(b)



(c)

**Figure 3.** The graph of X-ray diffraction pattern simulation with ionic radius of (a) MgO, (b) BaO and (c) ZnS.

MgO has a cubic structure with lattice parameters of  $a = 4.144 \text{ \AA}$  and Fm3m space group, while BaO has a tetragonal structure ( $a = b \neq c$ ) by adopting a space group P4 nmm. The ionic radius of cation ( $\text{Mg}^{2+}$ ) is smaller than the ionic radius of anion ( $\text{O}^{2-}$ ), while the ionic radius of cation

( $\text{Ba}^{2+}$ ) is greater than the ionic radius of ( $\text{Mg}^{2+}$ ) and is almost the same as the anion radius ( $\text{O}^{2-}$ ). Changes to the cation radius cause the transformation of the structure from Cubic ( $a = b = c$ ) to Tetragonal ( $a = b \neq c$ ). This structural change in BaO occurs because when ionic radii of cations and anions are almost the same then atoms tend to be arranged to form the structure with the largest density that can be formed, so BaO tends to have a tetragonal structure like a diamond structure. Similarly, ZnS has a cubic crystal system with ionic radius of  $\text{Zn}^{2+}$  cation that is quite different from the ionic radius of the  $\text{S}^{2-}$  anion atom.

Changes in the diffraction pattern in Figure 3 were then analyzed based on changes in the ionic radius of cation. The simulation graph of the pattern of diffraction peaks of the three compounds after being varied by the ionic radius of the atom is distinguished (+/-) by 0.1 Å from the standard size.

In general, changes in the size of the ionic radius of an atom cause the  $2\theta$  angle shift and a change in diffraction intensity. The effect of adding ionic radii causes  $2\theta$  angle shift towards the left (decreases) and the reduction in ionic radius causes a  $2\theta$  angle shift to the right (enlarged). This is in accordance with Bragg's Law which states that the angle value  $\theta$  will be inversely proportional to the lattice parameter, where the lattice parameter is proportional to the ionic radius.

#### 4 Conclusion

Simulation of the diffraction pattern of MgO, BaO and ZnS ceramic structures has been successfully conducted based on the results of the visualization. In dual atomic crystals, the size of the ionic fingers of the constituent atoms affects the shape of the structure possessed by a crystal. The effect of changes in ionic radius of constituent atoms causes changes in intensity and angular shifts of  $2\theta$ . The addition of ionic radii causes a  $2\theta$  angle shift to the left (shrinking). Moreover, the correlation of intensity with ionic radius cation does not have a uniform relationship due to the factors that affect X-ray scattering in crystals, namely multiplicity, Lorentz polarization factor, temperature and absorption factors.

#### REFERENCES

- [1] T. Surdia and S. Saito, *Pengetahuan Bahan Teknik*, Jakarta: Pradnya Paramita, 2005.
- [2] J. P. Glusker and K. N. Trueblood, *Crystal Structure Analysis: A Primer Third Edition*, United State: Oxford University Press Inc., 2010.
- [3] S. J. L. Billinge and I. Levin, "The Problem with Determining Atomic Structure at The Nanoscale," *Science*, vol. 316, no. 5824, pp. 561-565, 2007.
- [4] E. J. Mittemeijer and P. Scardi, *Diffraction Analysis of The Microstructure of Materials*, Germany: Springer-Verlag Berlin Heidelberg, 2004.
- [5] K. Thamaphat, P. Limsuwan and B. Ngotawornchai, "Phase Characterization of  $\text{TiO}_2$  Powder by XRD and TEM," *Kasetsart J.(Nat. Sci.)*, vol. 42, no. 5, pp. 357-361, 2008.
- [6] A. Monshi, M. R. Foroughi and M. R. Monshi, "Modified Scherrer Equation to Estimate



- More Accurately Nano-Crystallite Size Using XRD," *World Journal of Nano Science and Engineering*, vol. 2, no. 3, pp. 154-160, 2012.
- [7] V. A. Drits, J. Środoń and D. D. Eberl, "XRD Measurement of Mean Crystallite Thickness of Illite and Illite/Smectite: Reappraisal of The Kubler Index and The Scherrer Equation," *Clays and clay minerals* vol. 45, no. 3, pp. 461-475, 1997.
- [8] A. Beiser, *Fisika Modern*, Jakarta: Erlangga, 1995.
- [9] A. Guinier and G. Fournet, *Small-Angle Scattering of X-rays*, New York: John Wiley and Sons, Inc, 1955.
- [10] J. Epp, 4-X-Ray Diffraction (XRD) Techniques for Materials Characterization, In *Materials Characterization Using Nondestructive Evaluation (NDE) Methods*, pp. 81-124. Woodhead Publishing, 2016.
- [11] A. Chauhan and P. Chauhan. "Powder XRD Technique and Its Applications in Science and Technology." *Journal of Analytical and Bioanalytical Techniques*, vol. 5, no. 5, 212, pp. 1-5, 2014.
- [12] C. Kittel, *Introduction to Solid State* 7th ed., New York: John Willey and Sons Inc., 1986.
- [13] M. Ermrich and D. Oppel. "XRD for The Analyst Getting Acquainted with The Principles 2<sup>nd</sup> Edition, Nurnberger: PANalytical GmbH, 2013.
- [14] C. Suryanarayana and M. G. Norton, *X-Ray Diffraction A Practical Approach*, New York: Springer, 1998.
- [15] K. Momma and F. Izumi, "VESTA: A Three-Dimensional Visualization System for Electronic and Structural Analysis," *Journal of Applied Crystallography*, vol. 41, no. 3, pp. 653-658, 2008.
- [16] E. Angel and D. Shreiner, *Interactive Computer Graphics: A Top-Down Approach With Shader-Based OpenGL 6<sup>th</sup> Edition*, Boston: Addison-Wesley, 2012.
- [17] K. Momma and F. Izumi, "VESTA 3 for Three-Dimensional Visualization of Crystal, Volumetric and Morphology Data," *Journal of Applied Crystallography*, vol. 44, no. 6, pp. 1272-1276, 2011.
- [18] S. G. E. T. Escher, T. Lazauskas, M. A. Zwijnenburg and S. M. Woodley, "Structure Prediction of (BaO)<sub>n</sub> Nanoclusters for  $n \leq 24$  Using an Evolutionary Algorithm," *Computational and Theoretical Chemistry*, vol. 1107, pp. 74–81, 2017.
- [19] A. Kouchi, Y. Furukawa and T. Kuroda, "X-Ray Diffraction Pattern of Quasi-Liquid Layer on Ice Crystal Surface," *Journal de Physique Colloques*, vol. 48, pp. C1-675-c1-677, (1987).
- [20] S. S. Lobanov, Q. Zhu, N. Holtgrewe, C. Prescher, V. B. Prakapenka, A. R. Oganov and A. F. Goncharov, "Stable Magnesium Peroxide at High Pressure," *Scientific Reports*, vol. 5, 13582, pp. 1–8, 2015.